DESY 95-159
hep-ph/9508337
August 1995

ISSN 0418-9833

Dijet Cross Sections at $O(\alpha\alpha_s^2)$ in Photon-Proton Collisions

M. Klasen, G. Kramer
II. Institut für Theoretische Physik*
Universität Hamburg
D - 22761 Hamburg, Germany

Abstract

We have calculated inclusive two-jet production in low Q^2 ep collisions at $O(\alpha\alpha_s^2)$ superimposing direct and resolved contributions. The results are compared with recent experimental data from the ZEUS collaboration at HERA.

*Supported by Bundesministerium für Forschung und Technologie, Bonn, Germany under Contract 05 6HH93P(5) and EEC Program "Human Capital and Mobility" through Network "Physics at High Energy Colliders" under Contract CHRX-CT93-0357 (DG12 COMA)

1 Introduction

At HERA interactions between almost real photons and protons produce jets at high transverse momentum [1]. Due to the large momentum scale production cross sections should be calculable in perturbative QCD. In leading order (LO), i.e. in $O(\alpha\alpha_s)$, jet production proceeds through two distinct processes: (i) the virtual photon interacts directly with a parton in the proton (Fig. 1a) (direct component) or (ii) the virtual photon acts as a source of partons which collide with the partons in the proton (Fig. 1b) (resolved component). In the first case the full energy of the photon participates in the interaction and the fraction of the photon momentum x_γ involved in the hard scattering process is equal to one. In the resolved process, however, x_γ is always less than one. Another distinction is that in LO the final state in the resolved process includes a photon remnant in addition to two jets and the proton remnant whereas in the direct process the photon remnant is absent.

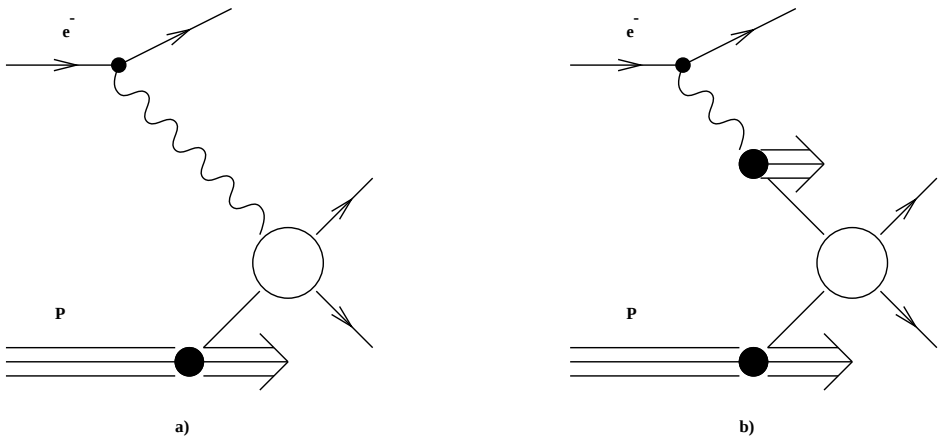

Figure 1: Schematic diagrams for a) direct and b) resolved photoproduction

In next-to-leading order (NLO) of α_s this distinction between direct and resolved contribution becomes ambiguous. Both components are related to each other through the factorization scale at the photon leg. The dependence of the NLO direct cross section on this scale must cancel to a very large extent against the scale dependence in the resolved cross section [2]. Higher order direct contributions can have a photon remnant. Furthermore, x_γ is no longer given in terms of the kinematical variables of the dijet system.

Recently the ZEUS collaboration [3] published an analysis of two-jet cross sections separating direct and resolved contributions with a cut on x_γ. They measured the dijet cross section as a function of the pseudorapidities of the two jets in regions which are sensitive to the gluon momentum density in the proton for large x_γ and sensitive to the gluon density in the photon for small x_γ. This procedure was suggested earlier by Forshaw and Roberts based on LO QCD calculations [4] which have also been used in the analysis of the ZEUS measurements.

Before information on the respective parton densities can be gained from such an analysis several important effects must be investigated in more detail. One of them is the influence of

NLO corrections to the direct and resolved photon cross sections on the comparison of the data with the theory. Such calculations exist for the inclusive single jet cross section for the direct [5, 6] and resolved cross sections [5, 7] separately which have been superimposed recently and compared to experimental data [8]. Bödeker also calculated the NLO direct inclusive two-jet cross section as a function of the two-jet invariant mass and the two jet rapidities [9]. For the comparison with the ZEUS data [3] the NLO calculations must be performed in such a way that the experimental constraints, in particular the cuts used to enrich the direct photon contribution, can be built in easily. Such a calculation for direct photoproduction in which the soft and collinear singularities of initial and final state are isolated by an invariant mass resolution cut has been completed recently by us [10]. Based on this work we have calculated the NLO inclusive cross section for direct photoproduction as a function of the average rapidity of the two jets and of the transverse energy. We have built in the experimental constraints on the kinematical variables as used in the ZEUS analysis. The contribution of the resolved photon in the enriched direct γ sample is estimated in LO since it is supposed to contribute only a fraction in this sample which is of interest for us. The effect of the NLO corrections of the resolved photon to this sample is left for future work.

In section 2 we shall define our direct photon dijet cross section and describe how it has been calculated. In section 3 we compare our results with the ZEUS measurements and discuss their relevance towards constraining the gluon distribution function of the proton at small x and the structure function of the photon for large x_γ, also with respect to the expectation of more accurate data in the future. We end in section 4 with our conclusions.

2 Direct Photon Dijet Cross Section

We have calculated the inclusive cross section for two-jet photoproduction coming from direct photons up to $\mathrm{O}(\alpha\alpha_s^2)$ for final states with at least two jets of $E_T > 6$ GeV. The photoproduction events are defined by those $ep \to eX$ scattering events where the Q^2 of the virtual photon is below $Q^2_{\max} = 4$ GeV^2. We describe the spectrum of the virtual photons by the Weizsäcker-Williams formula

$$zF_{\gamma/e}(z) = \frac{\alpha}{2\pi}(1 + (1-z)^2) \log\left(\frac{Q^2_{\max}(1-z)}{m_e^2\, z^2}\right) \tag{1}$$

where $z = E_\gamma/E_e$ is restricted to $0.2 < z < 0.8$ as in the ZEUS analysis. $E_e = 26.7$ GeV and $E_p = 820$ GeV.

We adopt the jet definition of the snowmass meeting [11] defining a jet as a collection of particles contained in a cone of radius $R = 1$ in the plane of rapidity and azimuthal angle around the jet momentum. This means that two partons may be considered as two separate jets or as a single jet depending whether they lie outside or inside the cone with radius R. In NLO the final state may consist of two jets or three jets. Then the three-jet sample consists of all $2 \to 3$ parton scattering contributions which do not fulfill the cone condition.

The cross section calculated is $\mathrm{d}\sigma/\mathrm{d}\bar{\eta}$ where $\bar{\eta} = \frac{1}{2}(\eta_1 + \eta_2)$ is the average rapidity of the two jets with the requirement that the difference of the rapidities $\eta^* = \eta_1 - \eta_2$ fulfills $|\eta^*| < 0.5$. This cross section is the integral of $\mathrm{d}^3\sigma/\mathrm{d}E_T\mathrm{d}\bar{\eta}\mathrm{d}\eta^*$ integrated over $E_T > 6$ GeV and $-0.5 < \eta^* < 0.5$.

The chosen E_T is the transverse energy of the so-called "trigger" jet with rapidity η_1 and η_2 is the rapidity of a second jet. The transverse energies of these two jets fulfill $E_{T_1}, E_{T_2} > E_{T_3}$. We note that $\bar{\eta}$ and $|\eta^*|$ are symmetric for $\eta_1 \leftrightarrow \eta_2$.

For $2 \to 2$ parton scattering energy and momentum conservation give the fraction of the photon energy participating in the hard scattering as

$$x_\gamma = \frac{E_T}{2zE_e}\left(e^{-\eta_1} + e^{-\eta_2}\right) \tag{2}$$

where zE_e is the initial photon energy and η_1 and η_2 are the rapidities of the two partons in the final state. If there were exclusively two jets in the final state, x_γ could be determined from their kinematical variables. The events with $x_\gamma = 1$ are exclusively direct production and those with $x_\gamma < 1$ resolved production. In NLO more than two jets are produced and $x_\gamma < 1$ is possible also for direct photoproduction. Therefore, in the ZEUS dijet analysis the observable x_γ^{OBS} was introduced, which is defined as the fraction of the photon energy participating in the production of the two highest E_T jets with variables E_{T_1}, η_1 and E_{T_2}, η_2 respectively:

$$x_\gamma^{\mathrm{OBS}} = \frac{1}{2zE_e}\left(E_{T_1}e^{-\eta_1} + E_{T_2}e^{-\eta_2}\right). \tag{3}$$

$x_\gamma^{\mathrm{OBS}} \leq x_\gamma$ since the x_γ in general has contributions from all jets produced which means

$$x_\gamma = \frac{1}{2zE_e}\sum_n E_{T_n}e^{-\eta_n} \tag{4}$$

where n runs up to $n = 3$ in NLO. In the x_γ^{OBS} distribution, nevertheless, we still expect the direct and resolved processes to populate different regions since the strictly two-jet samples of direct and resolved processes will dominate the cross section. Therefore, the direct processes are concentrated at large values of x_γ^{OBS}. The peak arising from the direct contribution will not necessarily lie at $x_\gamma^{\mathrm{OBS}} = 1$ due to higher order QCD effects. In the ZEUS analysis, direct and resolved photoproduction events are separated by a cut at $x_\gamma^{\mathrm{OBS}} = 0.75$. This value will also be used when we compare our results with the ZEUS data. For the case of only two jets in the final state we have $E_{T_1} = E_{T_2} \equiv E_T$, so that x_γ^{OBS} takes the following form when written in terms of $\bar{\eta}$ and η^*:

$$x_\gamma^{\mathrm{OBS}} = \frac{E_T}{zE_e}e^{-\bar{\eta}}\cosh\frac{\eta^*}{2}. \tag{5}$$

To select large x_γ^{OBS} it is necessary to choose $\bar{\eta} < 0$ for fixed E_T and $\eta^* \simeq 0$. The corresponding expression for the momentum fraction of the proton entering the hard scattering process is

$$x_p^{\mathrm{OBS}} = \frac{E_T}{E_p}e^{\bar{\eta}}\cosh\frac{\eta^*}{2} \tag{6}$$

so that x_p^{OBS} can be small if E_T is not too large. So for $E_T = 6$ GeV and $x_\gamma = 1$ we have $x_p \simeq 2 \cdot 10^{-3}$. Since the photon-gluon fusion $\gamma g \to q\bar{q}$ gives the dominant contribution, one is able to probe the gluon structure function of the proton to rather small values of x [4].

The theoretical framework of the calculation of the inclusive dijet cross section is the same as in reference [10, 12], where further details can be found. To cancel infrared and collinear

singularities present in the $2 \to 3$ matrix elements and in the virtual corrections to the $2 \to 2$ contributions, we apply the phase space slicing method which has also been applied to the calculation of jet production in e^+e^- collisions [13], γp collisions [14] and in deep inelastic scattering [15]. To separate the regions of phase space which contain the singularities, we introduce an invariant mass cutoff y. This cutoff is defined as usual with $s_{ij}/s < y$ where s_{ij} denotes the invariant mass squared of two particles i,j, and s is the partonic center of mass energy squared. Next we perform partial fractioning to isolate infrared and collinear singularities. Then we integrate the $2 \to 3$ cross sections over the phase space region with soft and collinear singularities up to the invariant mass cut. The remaining singularities which do not cancel among virtual and real corrections are absorbed by the usual factorization and renormalization into the parton densities of the photon and the proton. For sufficiently small values of y the relevant $2 \to 3$ subprocesses can be evaluated using an approximation where non-singular terms are neglected in order to facilitate the analytical integration over the soft and collinear regions of phase space. After this is done the remainder of the 3-body phase space contains no singularities. This procedure is particularly suited to build in kinematical constraints as used in the analysis of the experimental data.

The further calculation now is based on two separate contributions - a set of 2-body contributions and a set of 3-body contributions. Each set consists of finite parts, all singularities have been cancelled or subtracted and absorbed into structure functions. But each part depends separately on the cutoff y. In case that experimentally 2-jet and 3-jet cross sections could be measured with the same definitions concerning the 2-jet and 3-jet part, they could be compared to these results and the y dependence of the different jet samples could be tested. In this work we are interested in cross sections which are sufficiently inclusive, and the separation with the invariant mass cutoff y is only a technical device. The dependence on y must cancel in the inclusive cross section. We checked this with the usual inclusive single-jet cross section and a jet definition based on the cone algorithm described above. Of course, the single-jet cross section now depends on the cone radius R. We found complete independence of y and perfect agreement with the earlier results of Bödeker [6] who used the subtraction method to cancel soft and collinear singularities. To achieve agreement we had to choose a rather small value of $y = 10^{-3}$. Similar studies for jet photoproduction using different cutoffs were performed by Baer et al. [14]. We also compared with the two-jet invariant mass cross section in ref. [9] and found good agreement.

To be able to compare with the ZEUS measurements [3] we calculated the inclusive two-jet cross section $\mathrm{d}\sigma/\mathrm{d}E_T\mathrm{d}\bar{\eta}\mathrm{d}\eta^*$ for $|\eta^*| < 0.5$ and integrated over $E_T > 6$ GeV where E_T is the transverse energy of the "trigger" jet. The result as a function of $\bar{\eta}$ is shown in Fig. 2. In these curves no cut on x_γ^{OBS} is applied. The cross sections are for all direct contributions in LO (where $x_\gamma^{\mathrm{OBS}} = 1$) and in NLO with no additional constraints except those on η^* and E_T. As structure function for the proton we have chosen CTEQ3M [16], which is a NLO parametrization with $\overline{\mathrm{MS}}$ factorization and $\Lambda^{(4)} = 238$ MeV. This Λ value is also used to calculate the two-loop α_s value at the scale $\mu = E_T$. The factorization scale is chosen $M = E_T$ also. In Fig. 2 we show three curves. The full curve is the LO cross section with a maximum near $\bar{\eta} = 0$ and which is around 1.2 nb. The sharp drop-off near $\bar{\eta} = 0$ is caused by the constraints on z and on E_T. The other two curves are NLO results with $y = 10^{-3}$. The dashed curve is the genuine two-jet cross section containing the LO contribution and all terms of the three-parton final states with two partons having momenta in the cone with radius $R = 1$. This cross section

is negative due to y dependent terms ($\log y$ is dominant) which originate from the separation of the initial state singularities. Therefore, y acts as a physical cutoff which separates 2-jet contributions, where one of the partons is recombined with the remnant jets, from the genuine 3-jet contribution. Of course, when y takes a more physical (larger) value for this remnant recombination, the two-jet cross section becomes positive. The dotted curve shows the contribution of the 3-jet final state, which is positive and much larger than the LO prediction. This cross section depends also strongly on y due to the initial state singularities. The sum of 2-jet and 3-jet cross section gives 1.5 nb in the maximum and is independent of y, i.e. it is sufficiently inclusive to guarantee that the y dependence drops out.

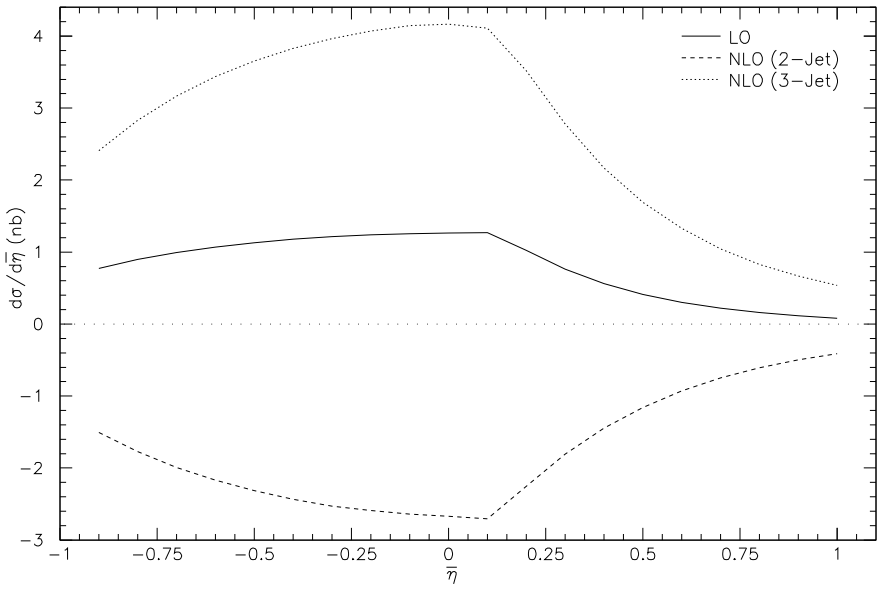

Figure 2: $\mathrm{d}\sigma/\mathrm{d}\bar{\eta}$ for $ep \to eX + 2$ (or more) jets for direct photoproduction with $E_T > 6$ GeV, $R = 1$ as a function of $\bar{\eta}$. The full curve is the LO cross section, the dashed (dotted) curve is the NLO 2-jet (3-jet) cross section with invariant mass cut $y = 10^{-3}$.

3 Comparison with ZEUS Data

Before we compare with the dijet cross sections as measured in the ZEUS experiment [3] we investigate the influence of the additional cuts on the NLO prediction. In these calculations we have taken $y = 10^{-3}$ in order to be independent on the approximations used in the analytical calculations. In the analysis of the ZEUS measurements the additional requirements are $x_\gamma^{\mathrm{OBS}} \geq 0.75$ to enhance the direct contributions and the constraint $E_{T_1}, E_{T_2} > 6$ GeV, i.e. the considered events contain at least two jets with equal minimal transverse energy. These two constraints influence the 3-jet cross section (dotted curve in Fig. 2) but not the 2-jet cross section (dashed curve in Fig. 2). Then immediately the problem arises whether the inclusive cross sections with these cuts are independent of y, i.e. are "infrared safe". Unfortunately, this is not the case due to y dependence of the cross sections originating from the initial state

collinear singularities.

The cut $x_\gamma^{\rm OBS} \geq 0.75$ modifies only the 3-jet contribution, which contains the 3-parton terms outside the cone radius R. Furthermore, the corrections to the 2-jet cross section originating from the initial state singularity at the photon leg have the same structure as a resolved cross section and have contributions for all x_γ, where x_γ is the fraction of the photon energy involved in the hard parton-parton scattering. If we separate the $x_\gamma \geq 0.75$ terms in this contribution, i.e. subtract the $x_\gamma < 0.75$ terms from the 2-jet cross section (dashed curve in Fig. 2), we obtain a NLO correction which is independent of y and coincides with the prediction with no cuts on x_γ. The result is shown as the dashed curve in Fig. 3.

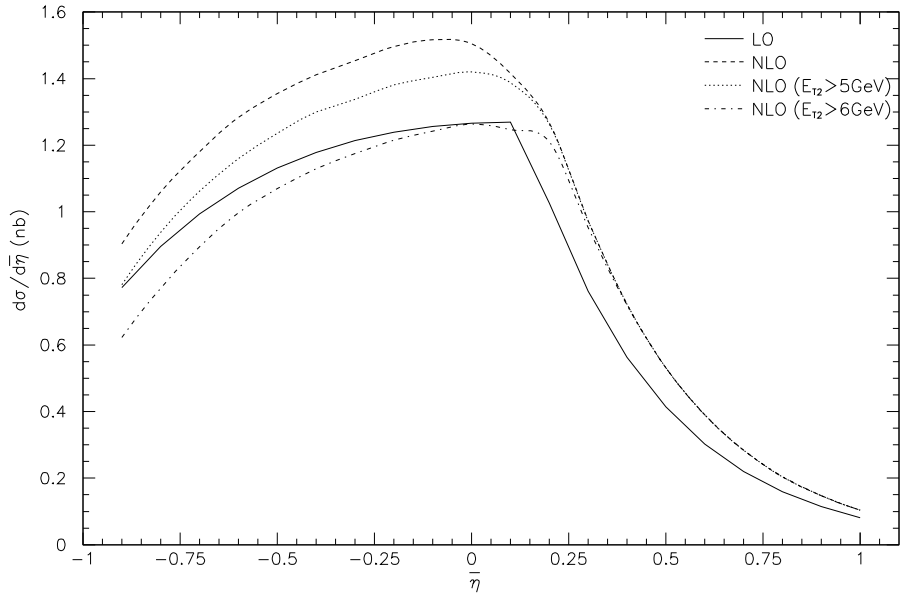

Figure 3: $\mathrm{d}\sigma/\mathrm{d}\bar{\eta}$ for NLO direct photoproduction with different constraints for the 3-jet contribution as a function of $\bar{\eta}$. The dashed curve is NLO from Fig. 2 with no constraints. The dotted (dot-dashed) curve is with $E_{T_1} > 6$ GeV, $E_{T_2} > 5$ GeV ($E_{T_1}, E_{T_2} > 6$ GeV, $E_{T_3} \lesssim 1$ GeV concerning 2- and 3-jet separation).

The experimental cut $E_{T_1}, E_{T_2} > 6$ GeV is more problematic since it also leads to cutoff dependent cross sections. With this strict cut on the E_T of both jets, there remains in some events very little transverse energy for the third jet, so that the y cut acts as a physical cut. If we arrange the 2- and 3-jet contributions in such a way that we introduce a cut on E_{T_3}, the transverse energy of the third jet, we obtain y cut independent NLO contributions again. We have introduced $E_{T_3} = 1$ GeV as a physical cut, where the contribution with $E_{T_3} < 1$ GeV is included in the two-jet cross section and the contribution $E_{T_3} > 1$ GeV is included in the three-jet cross section. With this additional constraint on the 3-jet part of the inclusive cross section we can demand $E_{T_1}, E_{T_2} > 6$ GeV. The result is the dot-dashed curve in Fig. 3, which we consider our final answer for the NLO direct cross section incorporating the ZEUS cuts. We see that it is almost the same as our LO prediction. This means that due to the various cuts the NLO correction is reduced very much. If we require only $E_{T_1} > 6$ GeV, $E_{T_2} > 5$ GeV we

also obtain a y-cut independent result. Then, the third jet can have enough transverse energy to compensate the initial state singularities. The cross section is 10% larger (dotted curve in Fig. 3) in this case.

The results in Fig. 3 do not include any tails, i.e. $x_\gamma \geq 0.75$ contributions, from the resolved cross section. This contribution has been estimated in [3] with the LO photon structure function of Gordon and Storrow [17] taking $E_T/2$ as the factorization scale and $\Lambda = 200$ MeV. This leads to a contribution of 0.15 nb in the maximum of $\mathrm{d}\sigma/\mathrm{d}\bar{\eta}$ for the resolved tail. To be consistent with our NLO calculations, we must choose a $\overline{\mathrm{MS}}$ NLO photon structure function. Then the resolved contribution for $x_\gamma \geq 0.75$ is much larger. In Fig. 4 we plotted this resolved cross section as a function of $\bar{\eta}$ for the photon structure functions GRV($\overline{\mathrm{MS}}$), GRV(DIS_γ) [18], GS(HO), which is NLO in the $\overline{\mathrm{MS}}$ scheme, and GS(LO, Set 2) [17], which was considered in [3], but now with scale $M_\gamma = E_T$ instead of $M_\gamma = E_T/2$ as used in the ZEUS analysis. Already this scale change increases the resolved contribution with GS(LO, Set 2) by 70%. In other words, the resolved cross section in the region $x_\gamma \geq 0.75$ is highly uncertain and can change by a factor of two, if different NLO photon structure functions are considered.

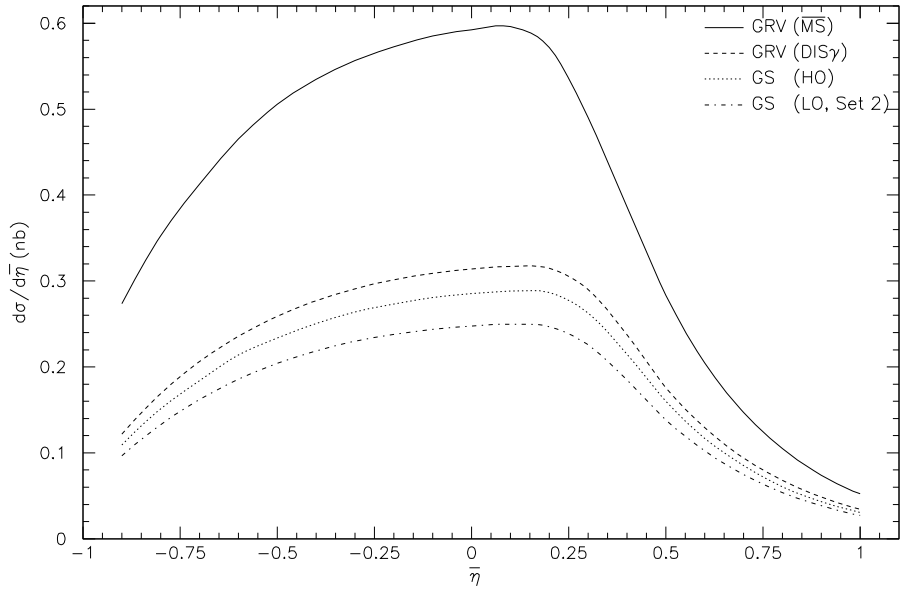

Figure 4: $\mathrm{d}\sigma/\mathrm{d}\bar{\eta}$ for LO resolved photoproduction using different photon structure function parametrizations as a function of $\bar{\eta}$.

In Fig. 5 we added the resolved cross sections with the GRV($\overline{\mathrm{MS}}$) and the GS(HO) structure functions to the NLO direct contribution from Fig. 3. The experimental points are from the ZEUS analysis where we corrected their cross sections for hadronization effects taken from their Fig. 3c. In addition, we added the energy scale uncertainty in quadrature to the combined statistical and systematic error. In Fig. 5 we see that our prediction combined with the NLO GS(HO) photon structure function reproduces the data very well. The prediction with the GRV($\overline{\mathrm{MS}}$) structure function is mostly above the data by a factor approximately 1.2, and it coincides approximately with the LO curve, which has been obtained by adding also

the resolved contribution with the GRV($\overline{\rm MS}$) structure function. This reflects the fact that in Fig. 3 the NLO direct cross section with all the cuts was not very different from the LO curve except for additional contributions in the $\bar{\eta} > 0$ region and a reduction in the $\bar{\eta} < 0$ region. We repeated the NLO calculation with the GRV photon structure function in the DIS$_\gamma$ scheme, which is by a factor of two smaller than the GRV function in the $\overline{\rm MS}$ scheme (see Fig. 4). For consistency, the subtracted terms in the photon structure function appear in the NLO direct cross section. Therefore the sum is not changed when we convert to the DIS$_\gamma$ scheme [2]. This has been checked explicitly, i.e. the NLO GRV curve is for the $\overline{\rm MS}$ and the DIS$_\gamma$ scheme. For this consistency it was essential that the resolved cross section which contains no NLO terms in the hard scattering is calculated with NLO proton and photon structure functions and with the same α_s, i.e. in two loops and with the same Λ value. LO structure functions and α_s in one-loop would also spoil the M_γ scale compensation between the NLO direct and resolved contributions.

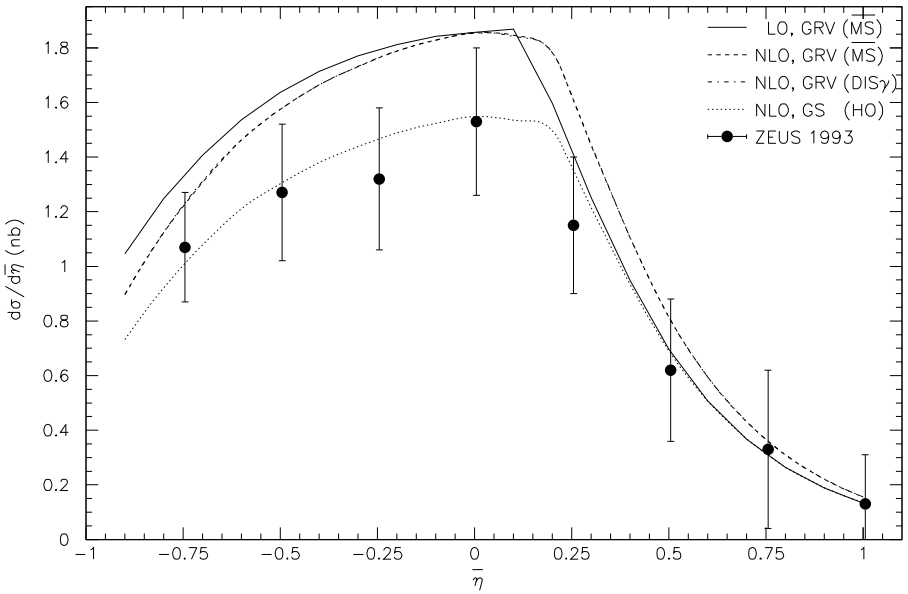

Figure 5: Sum of NLO direct and LO resolved cross sections $\mathrm{d}\sigma/\mathrm{d}\bar{\eta}$ as a function of $\bar{\eta}$ compared to data of ref. [3]. Four curves for different photon structure functions are shown: LO (full curve), NLO with GRV ($\overline{\rm MS}$ and DIS$_\gamma$) (dashed and dot-dashed), and NLO with GS (HO) (dotted).

From our analysis it is obvious that the resolved contribution to the two-jet cross section for $x_\gamma^{\rm OBS} \geq 0.75$ is not small. It can amount up to 50% of the direct contribution depending on the photon structure function. It appears that in the region $x_\gamma \geq 0.75$ the quark distribution of the GRV($\overline{\rm MS}$) structure function is much larger than for the GS(HO). The gluon part is small in this region. Indeed, for $Q^2 = 10$ GeV^2 the difference is approximately 50% [19]. At larger Q^2, which is relevant for our calculations, the difference must be even larger (see Fig. 5, compare with Fig. 4). Therefore, the inclusive two-jet cross section in the large x_γ region is suitable to obtain information on the quark distribution in the photon. By changing the boundary of the x_γ region towards $x_\gamma \to 1$ one might be able to establish whether the NLO quark distributions in the photon have the rather singular behaviour towards $x_\gamma \to 1$ as predicted by the GRV or

AFG functions [20], or if they behave more like in the GS structure function. We remark that a similar difference occurs in the LO GRV and GS structure functions [19]. But both change appreciably for $x_\gamma^{\rm OBS} \geq 0.75$, if one applies the NLO versions.

The two-jet cross section changes very little ($\simeq 0.1$ nb) when we use other proton structure functions which produce the existing deep inelastic data as well as CTEQ3M, as for example MRS(A'), MRS(G) [21],or GRV($\overline{\rm MS}$) [22]. This means, these structure functions all have more or less the same gluon distribution, which is very much determined by deep inelastic data and other data used in the analysis. Therefore, the direct part of the two-jet cross section is very well predicted by our NLO calculation and the emphasis is more on the resolved part in the large x_γ region.

Here our results are only an estimate since the NLO corrections are not included in the resolved cross section. From calculations of the inclusive one-jet cross sections it is known that these corrections for $R = 1$ are large taking LO results with NLO structure functions and two-loop α_s as the basis. This would enlarge the discrepancy of the predictions in Fig. 5 with the existing data even more for the GRV choice and may also lead to disagreement for the GS(HO) photon structure function.

Besides NLO corrections for the resolved part, there are other important topics which need further studies: the influence of possible jet pedestal energies on the data, the influence of hadronization and of incoming parton transverse momentum. The latter has been investigated for ingoing gluons in the direct cross section [23]. Its effect seems to decrease the direct cross section by approximately 0.3 nb [3], which might compensate for the larger resolved cross section with the GRV structure function in Fig. 4 and 5.

4 Conclusions

Differential dijet cross sections $\mathrm{d}\sigma/\mathrm{d}\bar{\eta}$ have been calculated in NLO for the direct and in LO for the resolved part as a function of $\bar{\eta}$. The kinematical constraints $|\eta^*| < 0.5$, $E_T > 6$ GeV, $0.2 < z < 0.8$, $Q^2_{\rm max} = 4$ GeV^2, $x_\gamma^{\rm OBS} \geq 0.75$, and $R = 1$ have been incorporated as in the ZEUS experiment. The cross sections have been obtained with the phase space slicing method for cancelling soft and collinear divergences in NLO. The infrared stability and the independence of the factorization scheme and scale at the photon leg have been tested. It turns out that the final result depends very much on the choice of the photon structure function for the resolved part. We think that the direct part is reliably predicted in NLO. Therefore measurements of the dijet cross sections in the large x_γ region offer the possibility to get information on the quark distribution of the photon near $x_\gamma = 1$.

References

[1] T. Ahmed et al., H1 Collaboration, Phys. Lett. B297 (1992) 205,
M. Derrick et al., ZEUS Collaboration, Phys. Lett. B297 (1992) 404,
I. Abt et al., H1 Collaboration, Phys. Lett. B314 (1993) 436,
M. Derrick et al., ZEUS Collaboration, Phys. Lett. B322 (1994) 287,
M. Derrick et al., ZEUS Collaboration, Phys. Lett. B342 (1995) 417,
T. Ahmed et al., H1 Collaboration, Nucl. Phys. B445 (1995) 195.

[2] D. Bödeker, G. Kramer, S.G. Salesch, Z. Phys. C63 (1994) 471.

[3] M. Derrick et al., ZEUS Collaboration, Phys. Lett. B348 (1995) 665.

[4] J.R. Forshaw, R.G. Roberts, Phys. Lett. B319 (1993) 539.

[5] L.E. Gordon, J.K. Storrow, Phys. Lett. B291 (1992) 320.

[6] D. Bödeker, Phys. Lett. B292 (1992) 164.

[7] G. Kramer, S.G. Salesch, Z. Phys. C61 (1994) 277.

[8] M. Klasen, G. Kramer, S.G. Salesch, DESY 94-232,
P. Aurenche, J.-Ph. Guillet, M. Fontannaz, Phys. Lett. B338 (1994) 98.

[9] D. Bödeker, Z. Phys. C61 (1994) 277.

[10] M. Klasen, G. Kramer, in preparation.

[11] J.E. Huth et al., Proc. of the 1990 DPF Summer Study on High Energy Physics, Snowmass, Colorado, edited by E.L. Berger, World Scientific, Singapore, 1992, p. 134.

[12] M. Klasen, Diploma Thesis, University of Würzburg, 1993.

[13] K. Fabricius, G. Kramer, G. Schierholz, I. Schmitt, Z. Phys. C11 (1982) 315,
F. Gutbrod, G. Kramer, G. Schierholz, Z. Phys. C21 (1984) 235,
G. Kramer, B. Lampe, Fortschr. Phys. 37 (1989) 161.

[14] H. Baer, J. Ohnemus, J.F. Owens, Phys. Rev. D40 (1989) 2844.

[15] D. Graudenz, Phys. Lett. B256 (1991) 518,
T. Brodkorb, J. G. Körner, Z. Phys. C54 (1992) 519,
D. Graudenz, Phys. Rev. D49 (1994) 3291.

[16] H.L. Lai et al., CTEQ Collaboration, Phys. Rev. D51 (1995) 4763.

[17] L.E. Gordon, J.K. Storrow, Z. Phys. C56 (1992) 307.

[18] M. Glück, E. Reya, A. Vogt, Phys. Rev. D46 (1992) 1973.

[19] A. Vogt, Proc. of the Workshop on Two-Photon Physics at LEP and HERA, Lund, eds. G. Jarlskog and L. Jönsson, Lund Univ., 1994, p. 141,
A. Vogt, private communication.

[20] P. Aurenche, M. Fontannaz, J.-Ph. Guillet, Z. Phys. C64 (1994) 621

[21] A.D. Martin, W.J. Stirling, R.G. Roberts, Phys. Rev. D51 (1995) 4756,
A.D. Martin, W.J. Stirling, R.G. Roberts, Phys. Lett. B354 (1995) 155.

[22] M. Glück, E. Reya, A. Vogt, Z. Phys. C67 (1995) 443.

[23] J.R. Forshaw, R.G. Roberts, Phys. Lett. B335 (1994) 494.